On the OTHER Hand: A Bilateral, Reconfigurable Hand Exoskeleton with Opposable Thumbs for Use with Upper Limb Exoskeletons

Peter Walker Ferguson, Jianwei Sun, Ji Ma, Joel Perry, and Jacob Rosen

This study aims to document the design of the OTHER Hand: a novel bilateral, reconfigurable, hand exoskeleton with opposable thumbs for use with upper limb exoskeletons. Intended for grasp research and rehabilitation with an emphasis on stroke, the OTHER Hand is designed as a one-size-fits-all system that can enable most of the common prehensile grasps and hand postures performed in activities of daily living. The capacity of the system to perform such grasps and postures is experimentally demonstrated by an average 94% normalized Grasping Ability Score across thirteen subjects using the Anthropomorphic Hand Assessment Protocol. This score demonstrates near-unhindered grasping performance for individuals without hand impairments wearing the OTHER Hand.

***Index Terms*—Exoskeletons, Rehabilitation robotics, Grasping, Hands, Design**

I. Introduction

Since the MIT-Manus in the early 90's [1], rehabilitation robots have been shown to be comparable to, and sometimes even superior to, human physical therapists [2]. While initial rehabilitation robots were nearly exclusively of the "end-effector" variety, anthropomorphic exoskeleton systems were developed and explored as potentially superior alternatives. These systems generally aim to be kinematically similar to the human body, and attach at several points for coordinated control of multiple joints of a limb, which is desirable for rehabilitation. To date, hundreds of exoskeletons have been developed for a variety of body parts and applications; those for the hand have been summarized in numerous review papers [3], [4], [5], [6], [7]. Despite the plethora of exoskeletons designed for the hand, there are few with sufficient *degrees of freedom* (DoFs) to enable the majority of grasp types that can also mount on arm exoskeletons. Two examples of such systems are the DEXO [8] and the NESM whole-arm exoskeleton [9], [10].

For individuals suffering from movement disability due to stroke, spinal cord injury, or other pathologies, it has been found that task-oriented rehabilitation is helpful for arm-hand strength, motor control, and function recovery [11]. However, these benefits are task specific, and related but untrained tasks see diminished improvements [11]. As such it is suggested that a variety of tasks should be trained and that random ordering of the tasks trained is preferred as it increases retention of performance improvements [11], [12]. Together, these require that exoskeletons for rehabilitation of the hand should have sufficient and appropriate DoFs to actuate the variety of grasps encountered in *activities of daily living* (ADLs). A key motion for enabling the multitude of grasps is thumb opposition. Indeed, it has been argued that "thumb opposition is required for all useful prehension" [13], and it is widely accepted that having opposable thumbs is what enables humans (and more broadly, primates) to grasp objects and use tools.

The exact kinematics of the thumb is still an active area of research, and models continue to be proposed [14]. Two common kinematic models of the thumb are used: one, more anatomically-based, places non-orthogonal, non-intersecting DoFs for *abduction/adduction* (A/A) and *flexion/extension* (F/E) at each of the *carpometacarpal* (CMC) and *metacarpophalangeal* (MCP) joints, and a F/E DoF at the interphalangeal joint as seen in [15], [16]; and the "surgeons' method," simpler, places a spherical joint at the CMC joint and only F/E at the MCP and interphalangeal joints [17]. Due to its simplicity, and assignment of the opposition motion to a single axis of rotation through the CMC as presented in [18], the surgeons' method is used in this study.

The A/A and *opposition/reposition* (O/R) motions of the thumb have multiple differing definitions in the literature. For clarity, we identify A/A as motion of the thumb tip away from/towards the plane of the palm without change in orientation of the plane of the thumbnail. O/R is defined as the circumduction of the thumb such that the plane of the thumbnail changes, with full opposition when the thumbnail is parallel to the frontal plane of the palm, and full reposition when the entire thumb is along the frontal plane of the palm. As described in [19], this motion is a complex combination of anatomical F/E, A/A, and rotation about the longitudinal thumb axis that is driven by thenar muscles.

Through visual inspection of thumb motions, it was approximated that O/R motions of the thumb can be obtained by rotation about a single axis through the CMC, parallel to the forearm when the wrist is neutral in F/E and radial/ulnar deviation as shown in Fig. 1A. A/A motions were found to be approximated by rotation about a perpendicular axis through the CMC that also lies in the plane of the palm when all fingers are extended.

While many hand exoskeletons in the literature include a thumb mechanism, most of them are only actuated in F/E. Of the remainders, the majority control A/A motions (as shown in Fig. 1A) [20], [21], [22], [23], [24], [25]. This is attributed to the ease of design of a DoF for A/A as the axis points

This work was supported by the National Science Foundation award #1532239. The content is solely the responsibility of the authors and does not necessarily represent the official views of the NSF.

Corresponding author: PWFerguson@ucla.edu, (240) 893-3884.

Peter Walker Ferguson, Jianwei Sun, Ji Ma, and Jacob Rosen are with the Department of Mechanical and Aerospace Engineering, University of California, Los Angeles, CA 90095 USA (e-mail: {pwferguson, sunjianw1, jima, jacobrosen}@ucla.edu).

Joel Perry is with the Mechanical Engineering Department, University of Idaho, Moscow, ID 83844 USA (e-mail: jperry@uidaho.edu).

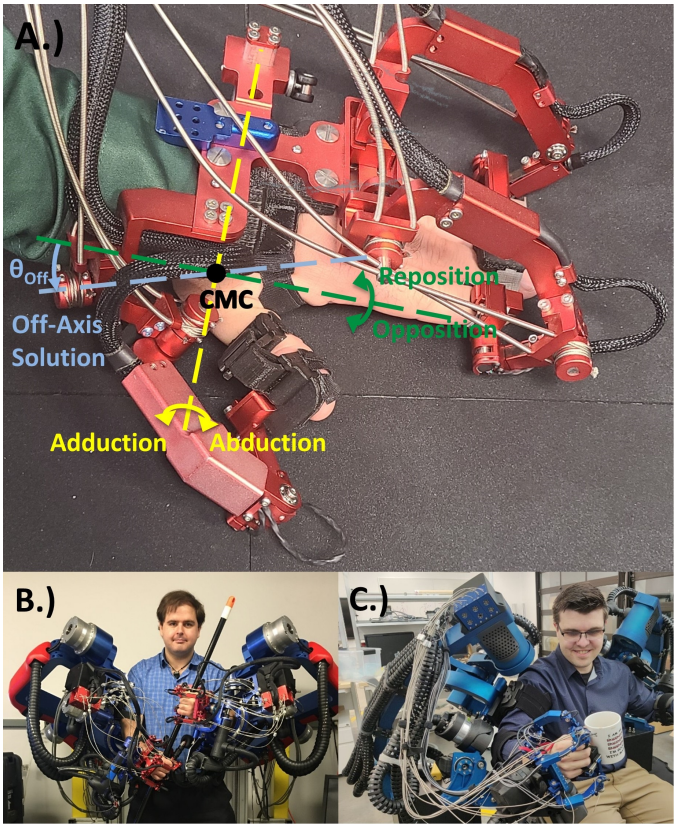

Fig. 1. The OTHER Hand: A.) With axes for A/A (yellow) and O/R (green) of the thumb for the CMC (black) modeled as a spherical joint and the off-axis DoF displayed in blue, B.) Mounted on the EXO-UL8 upper limb exoskeleton, C.) Mounted on the BLUE SABINO upper limb exoskeleton. The individuals depicted agreed to the use of their images.

out of the hand. It should be noted that the configuration of the thumb of these systems locks in varying degrees of opposition for grasping, but does not allow for active changing of said O/R angle. As such, each system may allow reposition grasps/postures (such as the lateral pinch or platform push) or opposition grasps (such as the pulp pinch or spherical grasp), but generally cannot do both and cannot be used to retrain the motions of O/R. Design of a mechanism for O/R (as shown in Fig. 1)A is complicated by proximity of the axis of rotation with the forearm. Additionally, radial deviation of the wrist moves the axis within the forearm, prohibiting any mechanism placed along the O/R axis for systems that do not constrain wrist deviation.

Several hand exoskeletons with O/R motions of the thumb have been developed. The mechanisms involved are generally either soft robot gloves or rigid robots with remote center-of-motion mechanisms. Soft robot gloves enable actuation of O/R without rigidly constraining movement and can relieve issues with axis misalignment. However, for individuals with pathologies of the hand, their muscles, tendons, and bones cannot be guaranteed to guide the motion along safe and useful trajectories. Furthermore, soft robot gloves often can only actuate each digit along a single predefined trajectory and must be reconfigured or re-manufactured for a different trajectory. Kadowaki et al. developed an entirely cloth and rubber soft robot glove using a spiral-type pneumatic rubber muscle to actuate O/R [26]. Polygerinos et al. developed a topologically similar glove that is portable and uses soft fiber-reinforced hydraulic actuators [27]. Maeder-York et al. created a thumb-only soft robot glove for task-oriented stroke rehabilitation therapy that used a fiber-reinforced actuator with elastomer wrapped in a strain layer to replicate the trajectory of the opposition grasp of an individual without hand impairment [28]. The FLEXotendon Glove-III is an assistive, voice-controlled, tendon-actuated thumb and two-finger silicone soft robot glove able to approximate thumb O/R [29]. The Maestro [30], [31] has a thumb kinematic chain with all F/E joints except the second, which intersects the CMC and is an A/A joint. However, because the axis of the A/A joint depends on the first joint's angle, the second joint effectively has an actively variable combination of A/A and O/R, though mostly A/A. Several generations of rigid hand exoskeletons with active thumb opposition have been developed at the BioRobotics Institute of Scuola Superiore Sant'Anna. The HANDEXOS approximated O/R with an axis placed on the dorsum of the hand driven by a slider-crank mechanism [32]. The HX is a rigid, cable-driven index finger and thumb exoskeleton that actuates O/R using an articulated parallelogram [18]. The HandeXos-Beta, or HX-β, iterates on the HX and features two actuated joints with incident axes coinciding with the CMC joint of the thumb that work in concert to enable thumb circumduction, series elastic actuators, and passive degrees of freedom for thumb and index internal/external rotation [33].

This study aims to describe, demonstrate, and validate the design of the *Opposable Thumb Hand Exoskeleton for Rehabilitation* (OTHER Hand). The OTHER Hand is a bilateral exoskeleton system with six-active and eight-passive DoFs of each hand, including active thumb O/R. The exoskeleton is mountable to the 7-DoF EXO-UL8 [34] and 9-DoF BLUE SABINO [35] upper limb exoskeletons, as in Fig. 1B and Fig. 1C, respectively, and is intended for grasp research and rehabilitation with an emphasis on stroke. Specifically, this study is intended to validate that a hand exoskeleton with the following design features enables the large majority of common prehensile grasp types:

1) An offset joint axis at the metacarpophalangeal thumb joint for opposition/reposition.
2) Three reconfigurable linkages.
3) A kinematically-optimized lateral base-to-distal topology.

In order to demonstrate the capabilities of the OTHER Hand, a validated test protocol for grasping of real world objects was desired. This is due to the intended use of the OTHER Hand as a rehabilitation device; it must be capable of training the grasps and hand postures needed for ADLs. Grasping of relevant physical objects enables tactile and kinesthetic feedback when performing rehabilitation tasks, which is shown to increase motor and functional recovery [36]. Furthermore, the abilities of the OTHER Hand should be tested for a range of user hand sizes to validate the design choices enabling it as a one-size-fits-all device. Several protocols for testing various metrics of hands (robotic, exoskeleton, and biological) have

been proposed, including applying Cutkowsky's Taxonomy [37] or the GRASP Taxonomy [38] (objects used are not standardized for either), the Action Research Arm Test [39] (also tests arm motions unrelated to hand design), or the Southampton Hand Assessment Procedure [40] (measures functionality based on task completion time, which is not inherent to the OTHER Hand design). Given the goal of evaluating grasping abilities but *not* arm manipulation (that is a factor of the upper limb exoskeleton to which the OTHER Hand attaches), the *Anthropomorphic Hand Assessment Protocol* (AHAP) was selected [41]. The AHAP is a systematic method of evaluating the ability of any system, be it robot prosthesis, biological hand, or human wearing a hand exoskeleton, to perform many of the common *Grasp types/hand postures* (GTs) used in ADLs with a variety of everyday objects. Further, it scores partially on the correctness of the GTs used. It was therefore deemed an ideal protocol for testing the OTHER Hand, as a high score would indicate that the exoskeleton could enable, and therefore likely help train in rehabilitation, the correct grasps used in ADLs on physical objects.

II. Design

The OTHER Hand was developed as a second-generation hand exoskeleton that can mount on upper limb exoskeletons. The design requirements are detailed in [42]; namely:

1) Low mass: mass at the hand must be minimized to reduce needed joint torques of the upper limb exoskeleton.
2) Torque: the actuators must enable forces on the digits of comparable magnitude to the maximum that an average adult operator can resist without moving.
3) Workspace: the workspace of the exoskeleton must contain the workspace of the human hand for relevant DoFs.
4) Grasp: the exoskeleton must be able to enable the large variety of grasps common to ADLs.
5) Open palm: the palm and fingers must be sufficiently unoccupied to permit interaction with physical objects.
6) Unisize: the system must be usable by 90% of the general population.

These requirements were addressed through a combination of a reconfigurable lateral "base-to-distal" topology, an opposable thumb mechanism, a kinematic link length optimization, easily donned/doffed finger and palm attachments, and remote location of motors via a Bowden cable transmission. Additional features include structurally integrated force sensors and a "pinky slider" mechanism.

A. Reconfigurable Topology

A reconfigurable lateral base-to-distal topology of three serial linkages that attach from the dorsal side of the hand to the distal phalanges addresses the workspace, grasp, open palm, and unisize requirements. Three linkages are used because all standard grasps can be accomplished with three or fewer "virtual fingers" [38]. The topology allows a one-size-fits-all design that neither requires adjustment for varying finger lengths nor impedes grasping most physical objects.

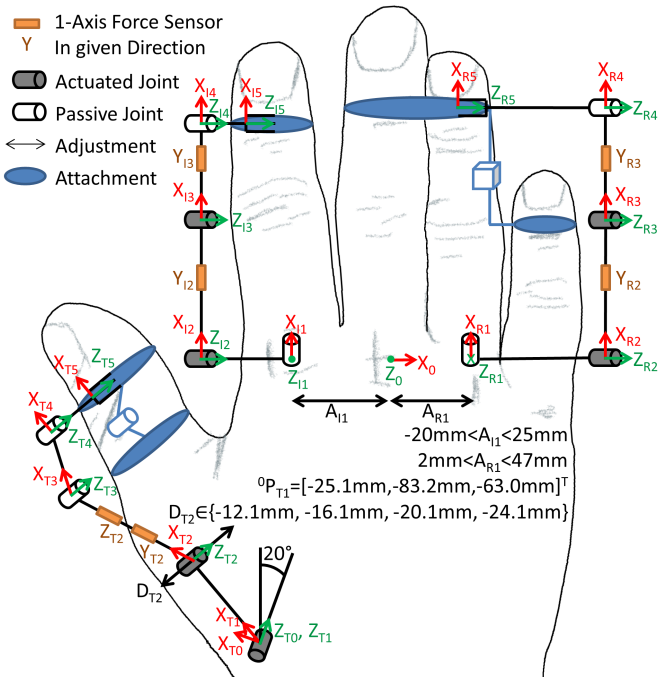

Fig. 2. Kinematics of the right OTHER Hand.

Fig. 2 shows the kinematics of the right OTHER Hand. The *Modified Denavit-Hartenberg* (DH) parameters and joint *ranges of motion* (ROMs) are provided in Tab. I. ROMs are defined with zero positions given by DH parameters, except θ_{I1} and θ_{R1} are 0° when A/A is neutral. Positive angles are defined for abduction, flexion, and opposition.

Each finger linkage consists of four serial DoFs. The first joint of each of the two finger linkages passively allows A/A motion. This DoF can be locked in the neutral A/A position. When unlocked, the range of motion is 25° from neutral towards abduction. All remaining joints are oriented for F/E of the associated finger(s), with the second and third joints actuated and the fourth passive. The final link is set to have zero link length. Together, each linkage passively allows A/A, actuates F/E to control distal phalanx position,

TABLE I
Modified DH Parameters of the Right OTHER Hand.

i	a_{i-1}	α_{i-1}	d_i	θ_i	θ_i ROM
$T1$	0	0	0	θ_{T1}	-20.7° — 236.8°
$T2$	31.9 mm	60°	D_{T2}	θ_{T2}	-19.3° — 206.8°
$T3$	83 mm	0	-2.5 mm	θ_{T3}	6.1° — 150°
$T4$	40 mm	0	0	θ_{T4}	0° — 360°
$T5$	0	0	24.1 mm	0	N/A
$I1$	A_{I1}	0	0	θ_{I1}	0° — 25°
$I2$	0	90°	-14.2 mm	θ_{I2}	-25.7° — 101.8°
$I3$	99 mm	0	-6.5 mm	θ_{I3}	3.4° — 173.6°
$I4$	40 mm	0	0	θ_{I4}	0° — 360°
$I5$	0	0	20.7 mm	0	N/A
$R1$	A_{R1}	180°	0	θ_{R1}	0° — 25°
$R2$	0	-90°	28.2 mm	θ_{R2}	-44.5° — 101.8°
$R3$	103 mm	0	6.5 mm	θ_{R3}	3.4° — 173.6°
$R4$	41 mm	0	0	θ_{R4}	0° — 360°
$R5$	0	0	-40.2 mm	0	N/A

and passively allows adjustment of orientation of the fingertip due to F/E. With positions specified, the kinematic constraints of the fingers largely prevent changing of orientation of the distal phalanges. The linkage that connects to the pinky finger features a passive "pinky-slider" mechanism to accommodate the pinky's large motion relative to the ring finger when flexing from an open palm to a fist.

A key feature of the OTHER Hand is reconfigurability of the linkages. The two finger linkages control all four fingers. One of the finger linkages is designed to always attach to the index finger, while the other always attaches to the ring and pinky fingers. Depending on which interchangeable finger attachments are used, the middle finger can be grouped with either linkage. This enables two configurations, denoted as 1-1-3 (thumb, index, middle+ring+pinky) as shown in Fig. 2, and 1-2-2 (thumb, index+middle, ring+pinky). Between the two configurations and the pinky slider mechanism, only grasps that require independent A/A motion of the pinky finger, such as a quadpod grasp [38], are prohibited. These grasps are used during less than 6% of the time spent in daily household tasks [43].

B. Opposable Thumb

The first-generation hand exoskeleton prototype demonstrated that just a 3R serial linkage for F/E of the thumb permitted too few grasps for ADLs. Thus, to better satisfy the grasp requirement, an additional DoF was added.

As the OTHER Hand is designed with a base-to-distal topology, the exoskeleton cannot individually control the anatomical A/A of the MCP and CMC. Instead, the added DoF should control the A/A or O/R of the entire thumb. It was determined that the ability to actuate O/R motions was of the highest priority due to the importance of opposition in grasping. It should be noted however, that although O/R motions are largely responsible for selecting between different grasp types (e.g. cylindrical versus lateral), A/A motions allow some fine tuning within grasp types (e.g. opposing the thumb to the index finger versus opposing the thumb to the pinky finger). Additionally, abduction is observed to almost only be useful when combined with opposition.

Initial designs for the O/R motion of the thumb attempted to solve the problem using a remote center of motion. However, these designs were deemed overly complex and prohibitively large for use with a hand exoskeleton to be placed on upper limb exoskeletons. Further, although O/R was achieved, the lack of any A/A created unnatural motion when tested with additively manufactured prototypes. As such, it was determined that moving the axis of rotation from O/R towards A/A by some angle θ_{Off}, as shown in Fig. 1A, could enable more natural motions. Furthermore, an off-axis design with sufficiently large θ_{Off} enables placement of the mechanism along the axis without interfering with radial deviation. As O/R was the primary desired motion, the minimum θ_{Off} that prevented this interference was chosen, namely 20°, to match normal radial deviation range of motion [44], [45]. Testing with 3D-printed prototypes confirmed the mechanism permitted opposition of all fingertips as well as full reposition.

The final thumb linkage design consists of four serial DoFs: the off-axis O/R joint followed by three rotary F/E joints. The first two joints are actuated, while the distal two are passive. As with the linkages for the long fingers, the final link has zero link length so that it only accommodates orientation changes. Although this underconstrains both the position and orientation of the thumb tip in the F/E plane, physical experiments verified that little passive motion is permitted due to the additional kinematic constraints imposed by the anatomy of the thumb.

C. Link Length Optimization

The unisize and workspace requirements dictate that the workspace of the OTHER Hand must cover the full relevant workspace of the hand, namely all reachable configurations of the fingers and thumb in their respective F/E planes, of all individuals between the 5th and 95th percentile for hand size. Due to the selection of a base-to-distal topology, this can be achieved without adjustments for link length if each linkage contains three F/E joints. However, an infinite number of link length combinations can satisfy these requirements. Thus, a design score is used to optimize the link lengths. This problem has been addressed by several hand exoskeletons with base-to-distal topologies [42], [46], [47]. The optimization algorithm used for the OTHER Hand is previously published in [48] and briefly summarized.

The optimization algorithm used a grid search for the optimal link lengths of each F/E link based on kinematic performance. As the exoskeleton must fit hands between the 5th and 95th percentiles for digit length, three sets of digits were optimized across representing those of 5th, 50th, and 95th percentile hand sizes. The lengths of each segment for each of the three digit sets were calculated from $\mu-2\sigma$, μ, and $\mu+2\sigma$, where μ and σ are the mean and standard deviation of each finger segment length as reported in [49]. For each of the three digit sets, the F/E joint angles were varied from 0° (extended without hyperextension) to fully flexed angles as reported in [50]. Combinations of possible mechanism link lengths were generated for each linkage. Elbow-up inverse kinematic solutions to all combinations of hand sizes and joint angles for the corresponding digit were calculated to obtain sets of joint angles $\boldsymbol{\theta}$, and all link length combinations without valid inverse kinematic solutions for the entire workspace were discarded. Remaining link length combinations were then given a design score based on high mechanism isotropy, $\mathrm{IS}(\boldsymbol{\theta})$, and low planar area of the polygon formed by the combined human finger-exoskeleton linkage system, $\mathrm{AR}(\boldsymbol{\theta})$, across the entire tested workspace of all three hand sizes:

$$\frac{\sum\limits_{\boldsymbol{\theta}\in K}(\mathrm{IS}(\boldsymbol{\theta}))\min\limits_{\boldsymbol{\theta}\in S}(\mathrm{IS}(\boldsymbol{\theta}))\min\limits_{\boldsymbol{\theta}\in M}(\mathrm{IS}(\boldsymbol{\theta}))\min\limits_{\boldsymbol{\theta}\in L}(\mathrm{IS}(\boldsymbol{\theta}))}{\sum\limits_{\boldsymbol{\theta}\in K}(\mathrm{AR}(\boldsymbol{\theta}))} \tag{1}$$

where S, M, L, and K are all combinations of $\boldsymbol{\theta}$ generated by link length and joint angle combinations of the small, medium, large, and all hands respectively. The first term in the numerator is the sum of the $\mathrm{IS}(\boldsymbol{\theta})$ across all configurations of the hands, and serves as proxy for the overall kinematic

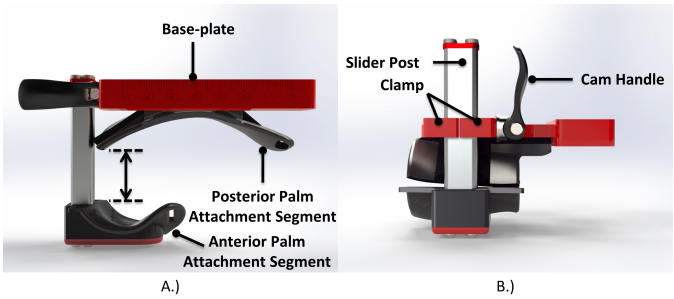

Fig. 3. Palm attachment. Note that hook-and-loop straps and neoprene padding are not displayed. A.) Front view with mechanism open. Arrows indicate the range of motion of the slider post. B.) Side view with mechanism closed.

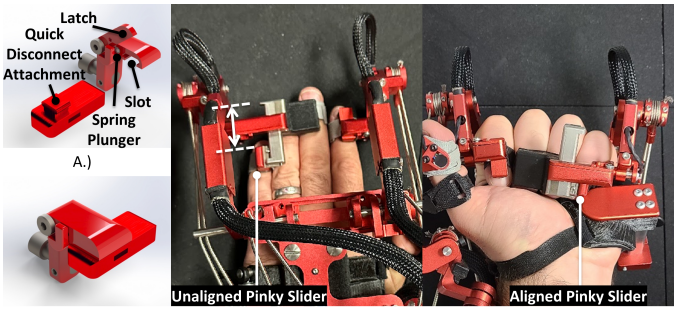

Fig. 4. Finger attachments. A.) Exploded view of the quick disconnect mechanism. B.) Assembled view. C.) Posterior view of the 1-1-3 finger attachments with pinky slider unaligned. Arrows indicate the range of motion of the pinky slider. D.) Anterior view with pinky slider aligned.

performance of the linkage. This is multiplied by the minimum $\mathrm{IS}(\boldsymbol{\theta})$ in the workspace of each of the small, medium, and large hands in order to penalize designs that do not perform well across all hand sizes. Lastly, the denominator consists of the sum of the $\mathrm{AR}(\boldsymbol{\theta})$ across all configurations of the hands in order to penalize designs that occupy excessive volumes. The set of link lengths with the highest design score for each digit was considered the optimal solution, as shown in Tab. II. They were tested with 3D-printed prototypes to verify kinematic performance and size, and were used in the OTHER Hand.

The lengths of the final links were set to zero to minimize the passive motion permitted by the distal-most joint. This necessitated placing the axis of rotation of the final joint lateral to the attachment point located 1cm distal to the distal-most joint. This resulted in negligible negative impact, in terms of obstructing interaction with physical objects, of also placing the first and second F/E joints lateral to the finger. This "lateral" base-to-distal topology removed the issue of joint collision between exoskeleton and biological fingers, which, in turn, allowed $\sim$30% shorter optimized linkages.

The kinematically optimized link lengths result in linkages with F/E planar workspaces fully covering those of biological hands with finger lengths between the 5th and 95th percentiles without hitting singularity. Full quantitative kinematic analysis is presented in [48].

D. Attachments

To assist ease of use by stroke patients, the OTHER Hand is designed to be quickly and securely donned/doffed. Following stroke, 42.6% of stroke patients develop some degree of spasticity [51], which presents in the hand as a sustained involuntary clench into a loose fist. Thus, a glove was ruled out, and the OTHER Hand was designed for each attachment to be donnable as independently as possible.

TABLE II
OPTIMIZED LINK LENGTHS.

Linkage	a_3 (mm)	a_4 (mm)	a_5 (mm)
Thumb	83	40	0
Index	99	40	0
Ring	103	41	0

The thermoplastic palm attachment is designed using 3D scans of a hand, and padded with neoprene where it contacts the user. It is separated into a posterior segment secured to the aluminum base-plate of the exoskeleton and an anterior segment connected to an aluminum sliding mechanism that can be quickly locked via a cam handle. Three sizes of the anterior segment are available for different hand sizes. To permit thumb O/R motions, the anterior segment only covers the proximal-ulnar portion of the palm. To further secure the palm, hook-and-loop straps connect between the anterior and posterior segments. The palm attachment is shown in Fig. 3.

To enable reconfigurability and ease of use, the thumb and all finger attachments are designed with quick disconnect mechanisms. Each attachment connects to the linkages by sliding into a slot and locking in place using a pivoting latch with a detent. Figs. 4A and 4B display the quick disconnect mechanism. The attachments are secured to the user's digits via hook-and-loop straps. The long-finger attachments attach to the distal phalanges just past the most distal joint. As the thumb actuates O/R, the attachment must be robust to rotation around the long axis of the thumb. Thus, the thumb attachment features a double parallelogram mechanism that attaches at both the distal and proximal phalanges and passively permits F/E of the interphalangeal joint.

In addition to enabling reconfigurability, the quick disconnect attachments make the device more easily donned by stroke patients. The quick disconnect mechanisms allow users to don the attachments finger-by-finger before getting into the exoskeleton. Once in the exoskeleton, each attachment can then be connected to the appropriate linkage. While wearing the finger attachments, a practiced user can insert the hand, secure the palm attachment, and connect the quick disconnects of one hand in approximately 45 seconds using their free hand. When fully attached, quick disconnects and palm attachments can be disconnected such that the hand can be removed from the exoskeleton in as little as 20 seconds.

The distal phalanx of the pinky frequently moves with respect to that of the ring finger. Specifically, with variation between individuals, the tip of the pinky distal phalanx can be several centimeters more proximal to the palm than that of the ring finger when the fingers are extended. However, when flexed into a fist, the pinky advances with respect to

the ring finger such that their tips align. To account for this, a pinky slider mechanism is incorporated in the attachments that connect to the ring and pinky fingers (and middle finger when in the 1-1-3 configuration). This slider mechanism constrains the pinky distal phalanx to be parallel to the ring distal phalanx, but allows it to move with a passive prismatic DoF. This permits approximation of most grasps requiring independent motion of the pinky finger that would otherwise be prohibited by a 1-2-2 or 1-1-3 configuration. The pinky slider is shown in Figs. 4C and 4D.

E. Actuation and Transmission

The OTHER Hand is actuated by Maxon motor combinations consisting of DCX19S GB KL 18V motor, GPX19HP 231:1 planetary gearhead, and ENX16EASY 256IMP incremental encoder. Geared brushed DC motors were selected due to their ease of control, reduced wire count, price, and performance. The actuators were sized to be powerful enough to apply meaningful resistive/assistive forces but not overly strong as to potentially harm the operator, force sensors, or Bowden cables. Based on observations of the first generation hand exoskeleton that featured motors with 0.3Nm nominal torque, which were an attractive size but incapable of applying adequate force, the OTHER Hand actuator combinations were selected to nominally provide 1.6Nm of torque. This translates to a maximum force of at least 11.1N applied on the distal phalanges in any direction in the F/E plane across the robot workspace. This is comparable to the maximum forces that the fingertip can resist without moving for individuals without hand impairments, which is highly dependent on finger position and force direction, as reported in [52].

For the torque and low mass requirements, a Bowden cable transmission enables remote placement of the motor pack, such as at the elbow joint of the EXO-UL8 or shoulder of the BLUE SABINO as seen in Fig. 1B and Fig.1C, reducing mass at the hand and permitting the use of actuators with sufficient torque for hand rehabilitation. The measured mass of the exoskeleton without the motor pack is 1.0kg. The cables used are CB-0044-777-CS-U steel 7x7x7 construction, 0.044" diameter wires with 756N breaking strength from Strand Products. The cables are sheathed in SG-100-023-120 0.1" outer diameter, 0.054" inner diameter round wire spring guides from the D.R. Templeman Company. To minimize the resistance of the cable guides to finger movements, the guides are routed through channels in the axis of rotation of the first joints of the finger linkages. In-line cable tension adjusters are installed on each cable.

F. Sensors

Each hand of the OTHER Hand exoskeleton features six single-axis force sensors, six quadrature encoders, and four magnetic rotary encoders. The force sensors are S215 single-point load cells with 53.37N capacity from Strain Measurement Devices. Each sensor is integrated to create the physical structure of the links. Each of the finger linkages possesses two load cells measuring forces in the F/E plane placed between the first and second F/E joints, and between the second and third F/E joints. The thumb contains two force sensors placed perpendicularly to each other, just after the actuated F/E joint, in order to measure forces associated with F/E and O/R. These sensors can be used for monitoring/data recording, as well as inputs for admittance control. Placement of the force sensors and direction of measured force are indicated in Fig. 2. Each actuated DoF is measured in rotation using the quadrature encoders. All passive joints involved in F/E are measured with RM08 magnetic rotary encoders from Renishaw.

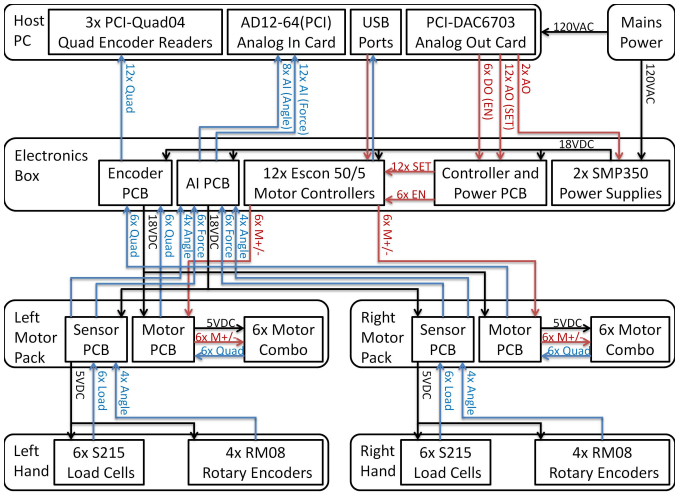

Fig. 5. Overview of the electronic subsystems and connections of the OTHER Hand. Red indicates outgoing command signals (towards the hand). Blue indicates incoming sensor signals (towards the host PC). Black indicates power signals.

G. Electronics and Control

The electronics of the OTHER Hand consist of four hubs: the host PC, the electronics box, and the left and right motor packs. Signal routing between hubs is displayed in Fig. 5.

The motor packs serve as the distal electronics hubs in order to improve wire management, reduce the length of cables including those for noise-sensitive unamplified force sensor signals, and amplify said signals. All sensor and motor signals are routed through custom PCBs at the motor packs.

The intermediate electronics hub is the electronics box. This rack mount enclosure contains the 12 ESCON 50/5 motor controllers from Maxon required to drive the actuators, two SMP350 18VDC 350W power supplies, and custom PCBs for wire routing. The front panel displays system status indicators, while the back panel contains the wiring interfaces to the motor packs, host PC, foot pedal, and emergency stop button. The foot pedal is a normally open momentary switch controlled by the user or therapist that acts as a safety feature to only enable actuators when pressed.

The host PC is a 4U rackmount industrial PC running Windows 10. On the PC are a PCI-DAC6703 analog output and three PCI-QUAD04 quadrature encoder reader PCI cards from Measurement Computing Corp., and an AD12-64(PCI) analog input PCI card from Contec. A 250Hz proportional-derivative admittance controller is implemented in C++. The admittance controller consists of six independent pairings of

force sensor with actuated joint. In the long fingers, each force sensor's measurement is input to the PD controller of the immediately proximal F/E joint. The thumb linkage force sensor measuring in the Y_{T2} direction provides input to the PD controller actuating the first thumb F/E joint while the sensor measuring in the Z_{T2} direction does so for the PD controller of the thumb O/R joint.

III. Experimental Evaluation of Grasping Ability

Most standardized performance tests of robotic hands attempt to quantify kinematic and dynamic capabilities or test very specific tasks, such as pick-and-place. Metrics such as workspace or actuation property comparisons to the human hand provide an overview of the anthropomorphism of the robot in terms of design specifications, however they do not address the ability to grasp real world objects [41]. Grasping ability is defined as the ability of the hand to both effectively initiate grasp and maintain a stable grip under motion without external forces [41]. The AHAP is designed to holistically measure the anthropomorphism of a robot hand operated by a human subject in terms of the ability to replicate the most characteristic grasp types used in ADLs with the standardized set of physical objects of varying physical characteristics in the *Yale-CMU-Berkeley Object Set* (YCB) [41], [53]. The AHAP is also generalizable across arbitrary robot hand systems, and thus enables comparison between different designs [41]. This permits the demonstration of grasping ability for the range of hand sizes of users of one-size-fits-all exoskeletons such as the OTHER Hand.

A. Procedure

10 GTs are tested with 25 objects across 26 tasks while wearing the OTHER Hand as shown in Fig. 6. The GTs tested in the AHAP are *pulp pinch or palmar pinch* (PP), *lateral pinch* (LP), *diagonal volar grip or adducted thumb grip* (DVG), *cylindrical grip* (CG), *extension grip* (EG), *tripod pinch* (TP), *spherical grip* (SG), *hook grip* (H), *platform* (P), and *index pointing/pressing* (IP). These grasps account for more than 90% of those performed by frequency of use, and the non-grasping postures are included due to their importance [41]. Each grasp is tested with three different objects of varying size, shape, weight, texture, and rigidity, and each non-grasp posture is tested with a single object, obtained from all categories of the YCB [41], [53]. Each task involves an operator demonstrating and instructing on a GT with the appropriate object before allowing a subject using the robotic hand to practice for one minute. The operator hands the object to the subject who then attempts to replicate the correct GT with palm pointing upwards. One point is obtained for holding/using the object with the correct GT, half a point for any other GT, and no points for failing to hold/use the object. The subject then naturally moves their arm/wrist to point the palm downwards and maintain the grip securely for three seconds. One point is obtained if the object does not move with respect to the hand, half a point if movement occurs but it is not dropped, and zero if the object is dropped. The platform position skips this second part of the test. The index pointing/pressing follows a different protocol, where a timer secured to a horizontal surface is pressed once and then again within three seconds with 1 point awarded for each press with the correct grasp, half a point for each with any other grasp, and zero if not pressed (or not pressed within 3 seconds for the second press). Each task is repeated three times for a maximum total *Grasping Ability Score* (GAS) of 153, which can be normalized as a whole or within GTs [41]. Inter- and intra- rater reliability, internal consistency, and responsiveness to small changes in robot hand design of the GAS have all been found to be high [41].

B. Clarifications

Clarifications by the authors are made to the AHAP procedure used.

- The initial pose (which is not specified by the AHAP) for each task is selected to be a closed fist with thumb opposed. This posture is selected to force users to pregrasp prior to grasping, further demonstrating the abilities of the OTHER Hand.
- The human hand within the OTHER Hand is considered for scoring purposes, and not the exoskeleton itself, with the exception of the palm of the OTHER Hand which is considered as part of the palm of the user. To do otherwise would prevent full scoring for many grasps despite correct posture of digits and secure grasp of the tested objects.
- A 1-1-3 finger configuration is used for the OTHER Hand as it enables all of the tested GTs based on scoring criteria.
- Last, all motors of the right OTHER Hand are actively controlled by the wearer throughout the protocol using the described admittance controller with zero desired force so that device transparency can be improved and the actuators, transmission, and controller can be subjectively tested across a range of users.

C. Subject Criteria

The experimental protocol was approved by the UCLA Office of the Human Research Protection Program with IRB#23-000035. Informed consent was received from all subjects.

Thirteen able-bodied subjects completed the protocol. Subjects were aged 24-34 (29.0±3.7, mean±standard deviation) with a 31%/69% female/male gender distribution. Of particular note was the distribution of hand sizes as approximated by length from the MCP to the tip of the distal phalanx of the index finger. The subjects measured 81.5±5.9mm, as compared to 81.8±10.3mm of the general population as found in [49]. Assuming a normal distribution, subjects ranged from the 10.5th to 80.5th percentiles in hand sizes.

IV. Results

The results of the AHAP testing of the OTHER Hand are displayed in Fig. 7. The mean and standard deviation for the GAS and GTs are listed in Tab. III. As one of the OTHER Hand's design goals is to be unisize, the GAS should remain high regardless of hand size.

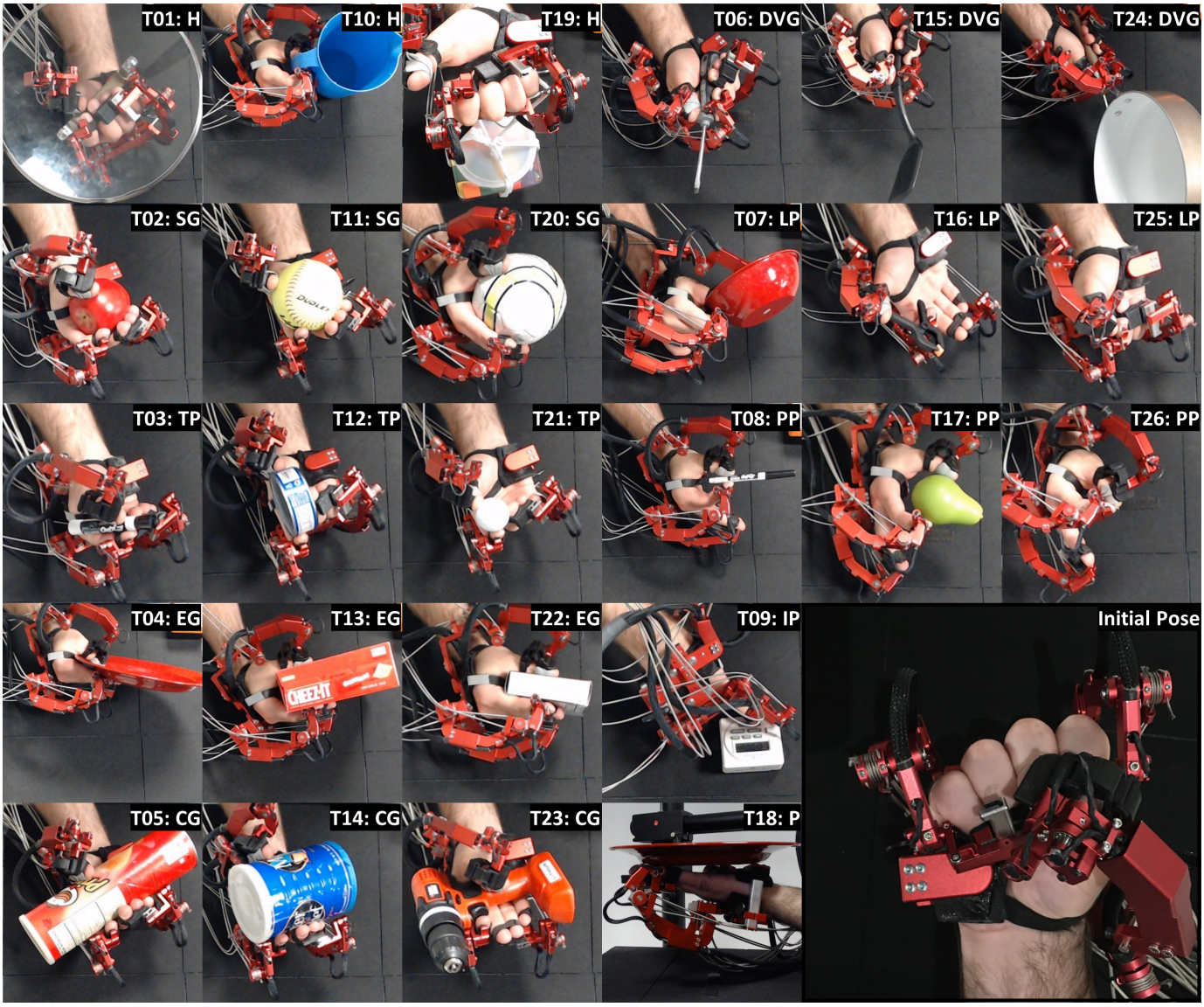

Fig. 6. All tasks of the AHAP and initial pose while wearing the OTHER Hand. Each task is labeled with task number and associated GTs. Note that the hand is angled for clearest viewing in photos, but all grasps are performed palm up.

Most users were able to correctly grasp and maintain for each task, as reflected by the average GAS of 143.79/153. However, two of the CG tasks and two of the LP tasks proved challenging, and the P task was performed with a caveat.

Task 14, which is grasping the coffee can with a CG, could generally be completed by all users with the correct grasp. However, the low-friction of the hook-and-loop straps used for the finger attachments and the high weight of the object caused the can to slip from some subjects' fingers when inverted for maintaining. This was particularly pronounced for users with smaller hands who relied on friction for a stable grasp.

TABLE III
SCORES BY GT.

GT	Mean	Std. Dev.	GT	Mean	Std. Dev.
GAS	143.79/153	5.31			
H	17.92/18	0.16	SG	17.13/18	1.18
TP	17.25/18	1.21	EG	17.29/18	0.82
CG	14.79/18	1.91	DVG	17.83/18	0.24
LP	15.54/18	1.56	PP	17.04/18	2.04
IP	6.00/6	0.00	P	3.00/3	0.00

Task 23, which is CG of the power drill, could not be correctly grasped by any user. This is due to the lateral base-to-distal topology of the OTHER Hand increasing the width of the four long fingers when placed together. The handle of the power drill is only long enough to fit a medium-sized user's hand, so the long finger linkages are blocked by the barrel of the drill and its battery pack. As such, no user was able to grasp the handle with contact between the object and the palmar side of all phalanges of at least three long fingers, as required. All users were able to make a similar grasp without such full contact, and could generally maintain the grasp.

Tasks 7 and 16 involve LP of the bowl and XS clamp, respectively. Both of these grasps were generally prevented due to placement of the index linkage on the radial side of the index finger. As such, the only unobstructed area of the index

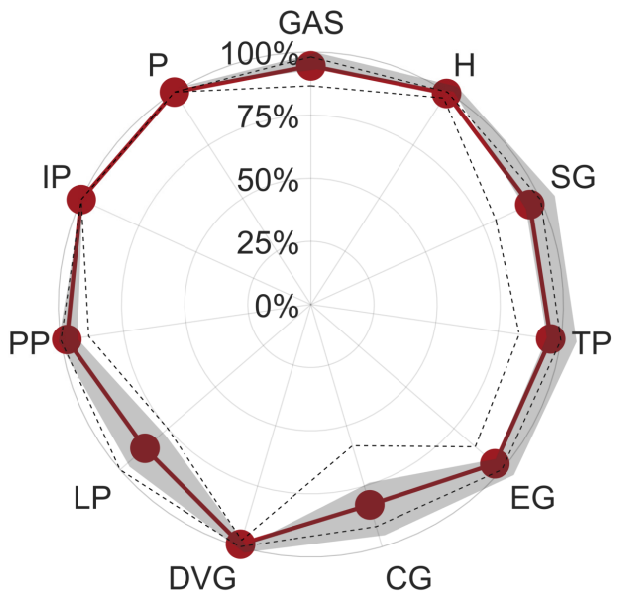

Fig. 7. Normalized overall scores by GTs. The solid line displays the mean across subjects, the dashed lines the maximum and minimum, and gray shaded area ± one standard deviation from the mean (which can exceed the maximum/minimum).

finger on the radial size was at the tip of the distal phalanx. Only some of the subjects with longer fingers could grasp the objects, albeit insecurely. Usually, subjects completed the tasks with PP or other similar grasps. It should be noted that LP of the key was not an issue due to its small size and the tendency for subjects to naturally grasp keys at the distal phalanx.

In addition, task 18 was performed unnaturally. All subjects made the correct posture given the criteria of the AHAP, and were able to hold up the plate. However, the plate rested on the exoskeleton, and did not make direct physical contact with the subject's hand as seen in Fig. 6. The score is therefore due to the inclusion of the palm attachment of the OTHER Hand as part of the palm for scoring purposes. Otherwise, all subjects would receive a half-score for this task.

The GAS of each subject is plotted against their hand size, as approximated by index finger length, in Fig. 8. While there is a moderate tendency for users with larger hands to score higher (Pearson correlation coefficient = 0.53), even the lowest-scoring subject scored a 132.5 (86.6%).

In addition to the traditional scoring metrics of the AHAP, the joint angles of the OTHER Hand were recorded. Of particular note to the evaluation of the design is the range of motion of the O/R joint. Large motions of the O/R joint in a task are indicative of the need for O/R to perform the required task starting from a closed fist posture. The minimum and maximum O/R joint angle across subjects for five representative tasks are shown in Fig. 9. It should be noted that, due to the base-to-distal topology, the O/R joint is the only joint angle directly comparable across users of varying hand sizes.

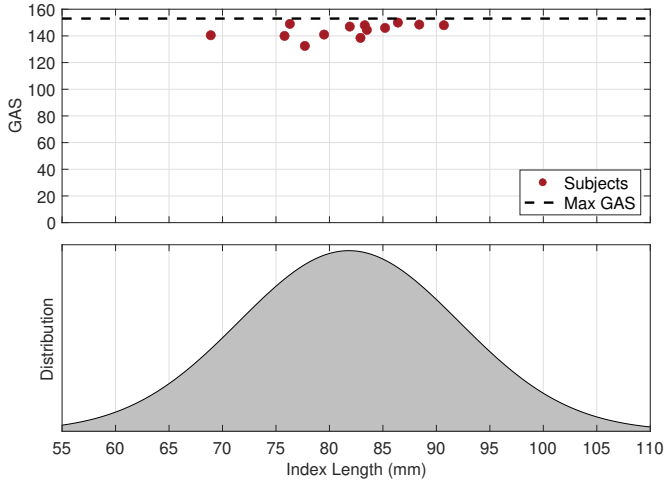

Fig. 8. GAS versus hand size of test subjects as approximated by index finger length. Index length of population is displayed for reference as a normal distribution with mean and standard deviation from [49]. Dashed line indicates max possible GAS.

V. Discussion

A. Grasping Ability Score

The high overall score of the OTHER Hand on the AHAP across all users indicates that the novel design choices resulted in a one-size-fits-all hand exoskeleton system capable of actuating the wide range of grasps needed for ADLs. The average normalized GAS of the OTHER Hand was 94.0%. This score is quite favorable compared to other systems found to have been tested with the AHAP in the literature. Various robotic hand and prosthetic systems report scores of 45-79% [41], [54], [55], [56]. The fabric-based soft ExHand Exoskeleton [57] scored 80.8% overall, with 65.8% for grasping and 95.8% for maintaining, excluding the T09:IP and T18:P tasks. All users could form all hand postures needed for the tasks, suggesting the OTHER Hand did not greatly hinder healthy grasping performance. Importantly, the novel thumb O/R axis enabled the subjects' desired thumb motions, and even surprised some subjects who were unaware the thumb linkage had fewer DoFs than the biological thumb. Subjects' comments in after-experiment discussions were also generally positive, particularly with regard to the ease, comfort, and naturalness of the permitted motions. It should be noted, however, that the high GAS is for wearers without hand impairments. Individuals with stroke or other impairments are anticipated to score much lower. Those with spasticity and tone would likely need active assistance to open their hand, and thus the score would be heavily dependent on the assistive control strategy used. Additionally, tissue volume and muscle belly differences in such populations may impact the security of the attachments and contact dynamics involved in the grasps.

B. Hand Size

It was determined that a 10th percentile hand is the smallest that could operate the OTHER Hand without constraining the thumb during simultaneous extension and opposition, in part due to the joint-stops preventing singularity. While not the

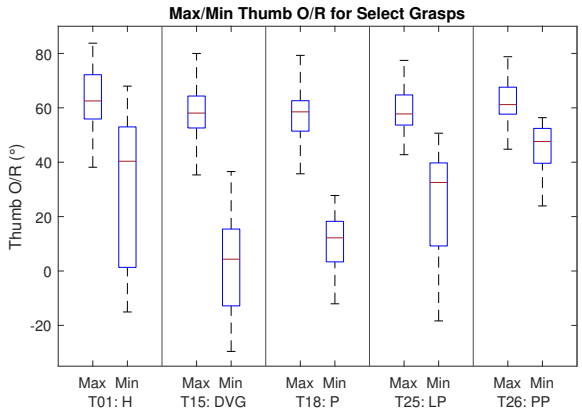

Fig. 9. Minimum and maximum thumb O/R angles measured across all subjects for five representative tasks.

5th percentile designed for, this is reasonable, as the link-length optimization accounted for F/E but not O/R motions that a single DoF can only approximate. Additionally, the experiments highlighted that lateral placement of the index linkage obstructed specific grasps for several objects, particularly for LP of large objects. For subjects with smaller hands, the linkages extended significantly distal to the fingertips when extended. Though this did not prevent grasp formation, it did require them to be careful with how they approached the object to avoid collision. These factors, along with the challenges of smaller hands grasping the coffee can in task 14, may give users with larger hands a slight advantage in GAS.

C. Attachments

Comfortable and secure finger attachments were previously identified as a challenge that was not satisfyingly solved, and this was highlighted in the evaluation. Two of the first five subjects expressed frustration with the thumb attachment slipping off, which was attached with just a hook-and-loop strap to the distal phalanx at the time. For the thumb, slipping may be partially due to kinematic overconstraint, as discussed in [58] as a single O/R DoF is used to approximate a complex multi-joint motion. Thus, the attachment was redesigned to a double parallelogram mechanism attached at both the distal and proximal phalanges, generally improving its security. Similarly, constraining independent motion of the pinky to a single DoF likely contributed to it slipping more than the other long fingers. While none of the tasks required splitting of the pinky from the ring finger, subjects may have attempted to move their pinky in such an independent manner regardless. It is speculated that alternate or additional passive couplings to the pinky finger could alleviate the slipping and better enable grasps requiring independent pinky motions. However, certain subjects were prone to slipping of finger attachments in general. These subjects tended to be those with more sharply tapered finger and thumb tips, which made it difficult to securely fasten the hook-and-loop straps without over-tightening and causing discomfort. Additionally, F/E motions were observed to cause small volume changes in the muscle belly, which caused the straps to slip. This may be of particular concern when using the OTHER Hand with stroke patients. Stroke is associated with both reduced muscle mass and volume, as well as increased intramuscular fat deposition [59]. As such, it is anticipated that contact dynamics with physical objects and attachment security may be impacted, but it is challenging to predict without physical evaluation of stroke patients wearing the OTHER Hand.

Feedback on and observations of the palm attachment throughout testing highlighted its strengths and weaknesses. It was easily and quickly donned and doffed for all users and provided a rigid connection to the hand as desired. It was far easier to don than a glove, and much more secure than only using straps. However, it was noted to be painful by several users when they repeatedly tensed their hands, as the rigid materials have very little give and constrained tissue. For others, the edges of the attachment dug into the palm. To address this, three different sizes of the anterior palm attachment segment were additively manufactured, and additional padding was added. These steps largely mitigated complaints. It is expected that future use of more compliant materials than polylactic acid will further improve comfort and possibly eliminate the need for multiple sizes while still maintaining the advantages compared to a glove or straps.

D. Importance of Opposition/Reposition

From Fig. 9, it can be seen that the importance of the O/R joint is task-dependent. Maximum O/R angle across all tasks were similar; this matches expectations due to tasks initiating with a clenched fist that requires an opposed thumb. However, the degree of reposition involved in tasks varied greatly. T01:H involved a hook grasp of the skillet lid that did not specify thumb behavior, consequently, different users selected widely varying O/R angles as was comfortable for them. T15:DVG and T18:P both required significant reposition to correctly perform their GTs. It is judged that these tasks were only able to be correctly performed (starting from a fist) because of the inclusion of an O/R joint. T25:LP and T26:PP, contrastingly, required minimal reposition of the thumb and instead mostly involved F/E. While the lateral pinch involved slightly more O/R motion than the pulp pinch, both tasks could likely be accomplished without a thumb joint for O/R.

E. Use of Bowden-Cable Transmission

The use of a Bowden-cable transmission has drawbacks in terms of elasticity and friction. Depending on cable routing and tension, the friction and stretch of the cables can create challenges with stiff position and impedance controllers. This may also impact the performance of assist-as-needed control strategies, where corrective feedback is provided when a subject is performing a task in a manner that is far from the desired, such as those discussed in [60], [61], [62]. However, the limitations on control were deemed justifiable given the advantages of the reduced mass and volume at the hand.

F. Potential Improvements to Clinical Practice

The experimental evaluation performed demonstrates that the OTHER Hand has significant ability to enable users to

perform the common grasps in ADLs. When combined with an assist-as-needed controller, which is the focus of future work, the system may serve as an effective rehabilitation tool for patients with hand impairments. When combined with an upper limb exoskeleton as intended, there is also the potential to enable full-arm reach to grasp task rehabilitation training, which has been shown to be more effective for recovery than just training individual motions [11].

G. Reconfigurability

The OTHER Hand was designed for use in rehabilitation, with a particular focus on stroke. From observations and the literature, stroke does not generally uniformly impair the different fingers of the hand [63]. Further, stroke patients often adopt compensatory grasping strategies using non-standard grasps and finger groupings [64]. As such, reconfigurability of the OTHER Hand to enable different finger groups of 1-1-3 or 1-2-2 is anticipated to widen its applicability as a rehabilitation device for stroke patients.

VI. Conclusion

The OTHER Hand is among the first bilateral, multi-DoF, rehabilitation hand exoskeleton systems designed for use with upper limb exoskeletons. It contains several notable features, including an opposable thumb, a lateral base-to-distal topology that is kinematically optimized to be unisize, quick disconnect attachments, and three reconfigurable linkages. The OTHER Hand's ability to perform a wide variety of grasps and hand postures with common household objects found in activities of daily living was experimentally demonstrated following the Anthropomorphic Hand Assessment Protocol. The design choices and features were validated by the average 94% normalized Grasping Ability Score. This score demonstrates near-unhindered grasping performance for individuals without hand impairments wearing the OTHER Hand, and indicates the potential of the system to train ADLs. However, the experiments also highlighted the need for continued development of secure, comfortable, and easy-to-use methods for attaching to fingers.

VII. Acknowledgements

The authors thank the late Frederick Schwedner, whose support and enthusiasm for the development of the OTHER Hand and EXO-UL8 were invaluable. Additional thanks to David Carrillo and Daniel Van Lewen for their assistance with assembly of the OTHER Hand.

References

[1] N. Hogan, H. I. Krebs, J. Charnnarong, P. Srikrishna, and A. Sharon, "MIT-MANUS : A Workstation for Manual Therapy and Training," in *IEEE Int. Workshop on Robot and Human Communication*, pp. 161–165, 1992.

[2] F. Molteni, G. Gasperini, G. Cannaviello, and E. Guanziroli, "Exoskeleton and end-effector robots for upper and lower limbs rehabilitation: Narrative review," *PM&R*, vol. 10, no. 9, Supplement 2, pp. S174–S188, 2018.

[3] M. A. Gull, S. Bai, and T. Bak, "A Review on Design of Upper Limb Exoskeletons," *Robotics*, vol. 9, no. 1, 2020.

[4] P. W. Ferguson, Y. Shen, and J. Rosen, "Hand Exoskeleton Systems–Overview," in *Wearable Robotics: Systems and Applications* (J. Rosen and P. W. Ferguson, eds.), pp. 149 – 175, Academic Press, 2020.

[5] M. Sarac, M. Solazzi, and A. Frisoli, "Design Requirements of Generic Hand Exoskeletons and Survey of Hand Exoskeletons for Rehabilitation, Assistive, or Haptic Use," *IEEE Transactions on Haptics*, vol. 12, no. 4, pp. 400–413, 2019.

[6] T. du Plessis, K. Djouani, and C. Oosthuizen, "A review of active hand exoskeletons for rehabilitation and assistance," *Robotics*, vol. 10, no. 1, 2021.

[7] P. Heo, G. M. Gu, S.-j. Lee, K. Rhee, and J. Kim, "Current Hand Exoskeleton Technologies for Rehabilitation and Assistive Engineering," *Int. Journal of Precision Engineering and Manufacturing*, vol. 13, no. 5, pp. 807–824, 2012.

[8] "DEXO: Dual Force-Feedback Arm and Hand Exoskeletons." https://www.spaceapplications.com/wp-content/uploads/2018/05/8-product-sheet-dexo-1.pdf, 2018. Accessed: 2023-04-15.

[9] C. Lauretti, F. Cordella, A. L. Ciancio, E. Trigili, J. M. Catalan, F. J. Badesa, S. Crea, S. M. Pagliara, S. Sterzi, N. Vitiello, N. Garcia Aracil, and L. Zollo, "Learning by Demonstration for Motion Planning of Upper-Limb Exoskeletons," *Frontiers in Neurorobotics*, vol. 12, p. 5, 2018.

[10] S. Crea, M. Nann, E. Trigili, F. Cordella, A. Baldoni, F. Badesa, J. M. Catalán, L. Zollo, N. Vitiello, N. Aracil, and S. Soekadar, "Feasibility and Safety of Shared EEG/EOG and Vision-Guided Autonomous Whole-Arm Exoskeleton Control to Perform Activities of Daily Living," *Scientific Reports*, vol. 8, 07 2018.

[11] A. A. Timmermans, H. A. Seelen, R. D. Willmann, and H. Kingma, "Technology-assisted training of arm-hand skills in stroke: concepts on reacquisition of motor control and therapist guidelines for rehabilitation technology design," *Journal of Neuroengineering and Rehabilitation*, vol. 6, no. 1, p. 1, 2009.

[12] J. W. Krakauer, "Motor learning: its relevance to stroke recovery and neurorehabilitation," *Current Opinion in Neurology*, vol. 19, no. 1, pp. 84–90, 2006.

[13] S. F. Duncan, C. E. Saracevic, and R. Kakinoki, "Biomechanics of the Hand," *Hand clinics*, vol. 29, no. 4, pp. 483–492, 2013.

[14] Y. Kawanishi, K. Oka, H. Tanaka, K. Okada, K. Sugamoto, and T. Murase, "In Vivo 3-Dimensional Kinematics of Thumb Carpometacarpal Joint During Thumb Opposition," *Journal of Hand Surgery*, vol. 43, no. 2, pp. 182.e1–182.e7, 2018.

[15] L. Y. Chang and Y. Matsuoka, "A Kinematic Thumb Model for the ACT Hand," in *IEEE Int. Conference on Robotics and Automation*, pp. 1000–1005, IEEE, 2006.

[16] D. Giurintano, A. Hollister, W. Buford, D. Thompson, and L. Myers, "A Virtual Five-Link Model of the Thumb," *Medical Engineering & Physics*, vol. 17, no. 4, pp. 297–303, 1995.

[17] A. I. Kapandji, "Clinical Evaluation of the Thumb's Opposition," *Journal of Hand Therapy*, vol. 5, no. 2, pp. 102–106, 1992.

[18] M. Cempini, M. Cortese, and N. Vitiello, "A Powered Finger-Thumb Wearable Hand Exoskeleton with Self-Aligning Joint Axes," *IEEE/ASME Transactions on Mechatronics*, vol. 20, no. 2, pp. 705–716, 2014.

[19] M. Tonkin, "Thumb Opposition: Its Definition and My Approach to Its Measurement," *Journal of Hand Surgery*, vol. 45, no. 3, pp. 315–317, 2020. PMID: 31793377.

[20] A. Wege and G. Hommel, "Development and Control of a Hand Exoskeleton for Rehabilitation of Hand Injuries," in *IEEE/RSJ Int. Conference on Intelligent Robots and Systems*, pp. 3046–3051, IEEE, 2005.

[21] M. Fontana, A. Dettori, F. Salsedo, and M. Bergamasco, "Mechanical Design of a Novel Hand Exoskeleton for Accurate Force Displaying," in *IEEE Int. Conference on Robotics and Automation*, pp. 1704–1709, IEEE, 2009.

[22] K. Tadano, M. Akai, K. Kadota, and K. Kawashima, "Development of Grip Amplified Glove Using Bi-Articular Mechanism with Pneumatic Artificial Rubber Muscle," in *IEEE Int. Conference on Robotics and Automation*, pp. 2363–2368, IEEE, 2010.

[23] P. M. Aubin, H. Sallum, C. Walsh, L. Stirling, and A. Correia, "A Pediatric Robotic Thumb Exoskeleton for At-Home Rehabilitation: the Isolated Orthosis for Thumb Actuation (IOTA)," in *IEEE Int. Conference on Rehabilitation Robotics*, pp. 1–6, IEEE, 2013.

[24] W. Chen, G. Li, N. Li, W. Wang, P. Yu, R. Wang, X. Xue, X. Zhao, and L. Liu, "Soft exoskeleton with fully actuated thumb movements for grasping assistance," *IEEE Transactions on Robotics*, vol. 38, no. 4, pp. 2194–2207, 2022.

[25] G. Li, L. Cheng, Z. Gao, X. Xia, and J. Jiang, "Development of an untethered adaptive thumb exoskeleton for delicate rehabilitation assistance," *IEEE Transactions on Robotics*, vol. 38, no. 6, pp. 3514–3529, 2022.

[26] Y. Kadowaki, T. Noritsugu, M. Takaiwa, D. Sasaki, and M. Kato, "Development of Soft Power-Assist Glove and Control Based on Human Intent," *Journal of Robotics and Mechatronics*, vol. 23, no. 2, pp. 281–291, 2011.

[27] P. Polygerinos, Z. Wang, K. C. Galloway, R. J. Wood, and C. J. Walsh, "Soft Robotic Glove for Combined Assistance and At-Home Rehabilitation," *Robotics and Autonomous Systems*, vol. 73, pp. 135–143, 2015.

[28] P. Maeder-York, T. Clites, E. Boggs, R. Neff, P. Polygerinos, D. Holland, L. Stirling, K. Galloway, C. Wee, and C. Walsh, "Biologically Inspired Soft Robot for Thumb Rehabilitation," *Journal of Medical Devices*, vol. 8, 04 2014.

[29] P. Tran, S. Jeong, F. Lyu, K. Herrin, S. Bhatia, D. Elliott, S. Kozin, and J. P. Desai, "Flexotendon glove-iii: Voice-controlled soft robotic hand exoskeleton with novel fabrication method and admittance grasping control," *IEEE/ASME Transactions on Mechatronics*, vol. 27, no. 5, pp. 3920–3931, 2022.

[30] P. Agarwal, Y. Yun, J. Fox, K. Madden, and A. D. Deshpande, "Design, Control, and Testing of a Thumb Exoskeleton with Series Elastic Actuation," *Int. Journal of Robotics Research*, vol. 36, no. 3, pp. 355–375, 2017.

[31] Y. Yun, Y. Na, P. Esmatloo, S. Dancausse, A. Serrato, C. A. Merring, P. Agarwal, and A. D. Deshpande, "Improvement of hand functions of spinal cord injury patients with electromyography-driven hand exoskeleton: A feasibility study," *Wearable Technologies*, vol. 1, p. e8, 2020.

[32] A. Chiri, N. Vitiello, F. Giovacchini, S. Roccella, F. Vecchi, and M. C. Carrozza, "Mechatronic Design and Characterization of the Index Finger Module of a Hand Exoskeleton for Post-Stroke Rehabilitation," *IEEE/ASME Transactions on Mechatronics*, vol. 17, no. 5, pp. 884–894, 2011.

[33] D. Marconi, A. Baldoni, Z. McKinney, M. Cempini, S. Crea, and N. Vitiello, "A novel hand exoskeleton with series elastic actuation for modulated torque transfer," *Mechatronics*, vol. 61, pp. 69–82, 2019.

[34] Y. Shen, P. W. Ferguson, J. Ma, and J. Rosen, "Upper Limb Wearable Exoskeleton Systems for Rehabilitation: State of the Art Review and a Case Study of the EXO-UL8—Dual-Arm Exoskeleton System," in *Wearable Technology in Medicine and Health Care* (R. K.-Y. Tong, ed.), pp. 71–90, Academic Press, 2018.

[35] P. W. Hill, E. T. Wolbrecht, and J. C. Perry, "Gravity Compensation of an Exoskeleton Joint Using Constant-Force Springs," in *2019 IEEE Int. Conference on Rehabilitation Robotics*, pp. 311–316, 2019.

[36] M.-A. Choukou, S. Mbabaali, J. Bani Hani, and C. Cooke, "Haptic-Enabled Hand Rehabilitation in Stroke Patients: A Scoping Review," *Applied Sciences*, vol. 11, no. 8, 2021.

[37] M. Cutkosky, "On Grasp Choice, Grasp Models, and the Design of Hands for Manufacturing Tasks," *IEEE Transactions on Robotics and Automation*, vol. 5, pp. 269–279, 06 1989.

[38] T. Feix, J. Romero, H.-B. Schmiedmayer, A. M. Dollar, and D. Kragic, "The GRASP Taxonomy of Human Grasp Types," *IEEE Transactions on Human-Machine Systems*, vol. 46, pp. 66–77, 02 2016.

[39] N. Yozbatiran, L. Der-Yeghiaian, and S. C. Cramer, "A Standardized Approach to Performing the Action Research Arm Test," *Neurorehabilitation and Neural Repair*, vol. 22, no. 1, pp. 78–90, 2008.

[40] C. M. Light, P. H. Chappell, and P. J. Kyberd, "Establishing a Standardized Clinical Assessment Tool of Pathologic and Prosthetic Hand Function: Normative Data, Reliability, and Validity," *Archives of Physical Medicine and Rehabilitation*, vol. 83, no. 6, pp. 776–783, 2002.

[41] I. Llop-Harillo, A. Pérez-González, J. Starke, and T. Asfour, "The Anthropomorphic Hand Assessment Protocol (AHAP)," *Robotics and Autonomous Systems*, vol. 121, p. 103259, 2019.

[42] P. W. Ferguson, B. Dimapasoc, Y. Shen, and J. Rosen, "Design of a Hand Exoskeleton for Use with Upper Limb Exoskeletons," in *Int. Symposium on Wearable Robotics*, pp. 276–280, Springer, 2018.

[43] J. Z. Zheng, S. De La Rosa, and A. M. Dollar, "An Investigation of Grasp Type and Frequency in Daily Household and Machine Shop Tasks," in *IEEE Int. Conference on Robotics and Automation*, pp. 4169–4175, IEEE, 2011.

[44] J. Ryu, W. P. Cooney, L. J. Askew, K.-N. An, and E. Y. Chao, "Functional Ranges of Motion of the Wrist Joint," *The Journal of Hand Surgery*, vol. 16, no. 3, pp. 409–419, 1991.

[45] D. C. Boone and S. P. Azen, "Normal Range of Motion of Joints in Male Subjects," *The Journal of Bone and Joint Surgery*, vol. 61, no. 5, pp. 756–759, 1979.

[46] N. Secciani, M. Bianchi, A. Ridolfi, F. Vannetti, Y. Volpe, L. Governi, M. Bianchini, and B. Allotta, "Tailor-Made Hand Exoskeletons at the University of Florence: From Kinematics to Mechatronic Design," *Machines*, vol. 7, no. 2, p. 22, 2019.

[47] M. Fontana, S. Fabio, S. Marcheschi, and M. Bergamasco, "Haptic Hand Exoskeleton for Precision Grasp Simulation," *Journal of Mechanisms and Robotics*, vol. 5, 10 2013.

[48] P. W. Ferguson, B. Dimapasoc, and J. Rosen, "Optimal Kinematic Design of the Link Lengths of a Hand Exoskeleton," in *Wearable Robotics: Systems and Applications* (J. Rosen and P. W. Ferguson, eds.), pp. 193 – 206, Academic Press, 2020.

[49] B. Alexander and K. Viktor, "Proportions of Hand Segments," *Int. Journal of Morphology*, vol. 28, no. 3, pp. 755–758, 2010.

[50] M. C. Hume, H. Gellman, H. McKellop, and R. H. Brumfield, "Functional Range of Motion of the Joints of the Hand," *Journal of Hand Surgery*, vol. 15, no. 2, pp. 240–243, 1990.

[51] P. P. Urban, T. Wolf, M. Uebele, J. J. Marx, T. Vogt, P. Stoeter, T. Bauermann, C. Weibrich, G. D. Vucurevic, A. Schneider, *et al.*, "Occurence and Clinical Predictors of Spasticity After Ischemic Stroke," *Stroke*, vol. 41, no. 9, pp. 2016–2020, 2010.

[52] R. Yokogawa and K. Hara, "Measurement of Distribution of Maximum Index-Fingertip Force in all Directions at Fingertip in Flexion/Extension Plane," *Journal of Biomechanical Engineering*, vol. 124, pp. 302–307, 05 2002.

[53] B. Calli, A. Walsman, A. Singh, S. Srinivasa, P. Abbeel, and A. M. Dollar, "Benchmarking in Manipulation Research: Using the Yale-CMU-Berkeley Object and Model Set," *IEEE Robotics Automation Magazine*, vol. 22, pp. 36–52, 09 2015.

[54] I. Llop-Harillo, A. Pérez-González, and J. Andrés-Esperanza, "Grasping Ability and Motion Synergies in Affordable Tendon-Driven Prosthetic Hands Controlled by Able-Bodied Subjects," *Frontiers in Neurorobotics*, vol. 14, 2020.

[55] L. Timm, M. Etuket, and S. Sivarasu, "Design and Development of an Open-Source ADL-Compliant Prosthetic Arm for Trans-Radial Amputees," vol. 2022 Design of Medical Devices Conference of *Frontiers in Biomedical Devices*, 04 2022.

[56] M. A. Bardien and S. Sivarasu, "The Self Actuated Tenim Hand: The Conversion of a Body-Driven Prosthesis to an Electromechanically Actuated Device," vol. 2021 Design of Medical Devices Conference of *Frontiers in Biomedical Devices*, 04 2021.

[57] J. C. Maldonado-Mejía, M. Múnera, C. A. R. Diaz, H. Wurdemann, M. Moazen, M. J. Pontes, M. E. Vieira Segatto, M. E. Monteiro, and C. A. Cifuentes, "A fabric-based soft hand exoskeleton for assistance: the ExHand Exoskeleton," *Frontiers in Neurorobotics*, vol. 17, 2023.

[58] A. Schiele and F. C. T. van der Helm, "Kinematic design to improve ergonomics in human machine interaction," *IEEE Transactions on Neural Systems and Rehabilitation Engineering*, vol. 14, no. 4, pp. 456–469, 2006.

[59] V. Azzollini, S. Dalise, and C. Chisari, "How Does Stroke Affect Skeletal Muscle? State of the Art and Rehabilitation Perspective," *Frontiers in Neurology*, vol. 12, 2021.

[60] L. L. Cai, A. J. Fong, C. K. Otoshi, Y. Liang, J. W. Burdick, R. R. Roy, and V. R. Edgerton, "Implications of assist-as-needed robotic step training after a complete spinal cord injury on intrinsic strategies of motor learning," *Journal of Neuroscience*, vol. 26, no. 41, pp. 10564–10568, 2006.

[61] M. Maaref, A. Rezazadeh, K. Shamaei, R. Ocampo, and T. Mahdi, "A bicycle cranking model for assist-as-needed robotic rehabilitation therapy using learning from demonstration," *IEEE Robotics and Automation Letters*, vol. 1, no. 2, pp. 653–660, 2016.

[62] P. Agarwal and A. D. Deshpande, "A framework for adaptation of training task, assistance and feedback for optimizing motor (re)-learning with a robotic exoskeleton," *IEEE Robotics and Automation Letters*, vol. 4, no. 2, pp. 808–815, 2019.

[63] E. T. Wolbrecht, J. B. Rowe, V. Chan, M. L. Ingemanson, S. C. Cramer, and D. J. Reinkensmeyer, "Finger strength, individuation, and their interaction: Relationship to hand function and corticospinal tract injury after stroke," *Clinical Neurophysiology*, vol. 129, no. 4, pp. 797–808, 2018.

[64] A. García Álvarez, A. Roby-Brami, J. Robertson, and N. Roche, "Functional classification of grasp strategies used by hemiplegic patients," *PLOS ONE*, vol. 12, pp. 1–21, 11 2017.